THE JOURNAL OF BIOLOGICAL CHEMISTRY VOL. 285, NO. 24, pp. 18759–18768, June 11, 2010

FATP1 Inhibits 11-*cis* Retinol Formation via Interaction with the Visual Cycle Retinoid Isomerase RPE65 and Lecithin:Retinol Acyltransferase*[S]

Received for publication, September 9, 2009, and in revised form, March 30, 2010 Published, JBC Papers in Press, March 31, 2010, DOI 10.1074/jbc.M109.064329

Thomas J. P. Guignard[‡], Minghao Jin[§], Marie O. Pequignot[‡], Songhua Li[§], Yolaine Chassigneux[‡], Karim Chekroud[‡], Laurent Guillou[‡], Eric Richard[¶], Christian P. Hamel[‡], and Philippe Brabet[‡‖1]**

*From the [‡]Inserm U583, Institut des Neurosciences de Montpellier, Montpellier, 34091 France, the [‖]University Montpellier 1, Montpellier, 34967 France, the **University Montpellier 2, Montpellier, 34095 France, the [§]Department of Ophthalmology, Neuroscience Center, Louisiana State University School of Medicine, New Orleans, Louisiana 70112, and the [¶]Centre de Biochimie Structurale CNRS UMR 5048-UM1-Inserm UMR 554, 29 rue de Navacelles, Montpellier, 34090 France*

The isomerization of all-*trans* retinol (vitamin A) to 11-*cis* retinol in the retinal pigment epithelium (RPE) is a key step in the visual process for the regeneration of the visual pigment chromophore, 11-*cis* retinal. LRAT and RPE65 are recognized as the minimal isomerase catalytic components. However, regulators of this rate-limiting step are not fully identified and could account for the phenotypic variability associated with inherited retinal degeneration (RD) caused by mutations in the *RPE65* gene. To identify new RPE65 partners, we screened a porcine RPE mRNA library using a yeast two-hybrid assay with full-length human RPE65. One identified clone (here named FATP1c), containing the cytosolic C-terminal sequence from the fatty acid transport protein 1 (FATP1 or SLC27A1, solute carrier family 27 member 1), was demonstrated to interact dose-dependently with the native RPE65 and with LRAT. Furthermore, these interacting proteins colocalize in the RPE. Cellular reconstitution of human interacting proteins shows that FATP1 markedly inhibits 11-*cis* retinol production by acting on the production of all-*trans* retinyl esters and the isomerase activity of RPE65. The identification of this new visual cycle inhibitory component in RPE may contribute to further understanding of retinal pathogenesis.

In vertebrates, vision begins in photoreceptors (rod and cone) with the absorption of light by the visual pigments, rhodopsin and cone opsins, which consist of two components: opsin (apoprotein) and 11-*cis* retinaldehyde (11*c*RAL,[2] chromophore). Light causes photoisomerization of 11*c*RAL to all-*trans* retinal (a*t*RAL) that dissociates from opsin. The a*t*RAL is reduced to all-*trans*-retinol (a*t*ROL, vitamin A), which is in turn converted to 11-*cis* retinol (11*c*ROL) and oxidized to 11*c*RAL in the neighboring retinal pigment epithelium (RPE). The whole process involves both retinoid transport proteins and enzymes and is termed the visual (retinoid) cycle (1–3).

In the RPE, a*t*ROL is first esterified in the smooth endoplasmic reticulum membrane by a lecithin:retinol acyltransferase, LRAT (4, 5), to fatty acids to form all-*trans*-retinyl-esters (a*t*RE). The latter are recognized by the RPE-specific protein RPE65 (MIM 180069) that catalyzes their cleavage and isomerization to the 11*c*ROL (6, 7). 11*c*ROL is then oxidized to 11*c*RAL by the 11*c*ROL dehydrogenase (11*c*RDH), a member of the short chain alcohol dehydrogenases (8). Cellular retinaldehyde-binding protein (CRALBP) is an abundant carrier of both 11*c*ROL and 11*c*RAL that facilitates the 11*c*ROL formation and its oxidation to 11*c*RAL (9, 10).

Isomerization is a rate-determining step in the visual cycle. In mice, the level of RPE65 expression is strain-dependent and determine the rate-limited rhodopsin regeneration (11, 12). Recently, *in vitro* assays have shown that multiple disease-associated mutations in human RPE65 shown to decrease protein concentration, directly affect the isomerase activity (13, 14). This rate-determining step may be regulated. For example, phosphate-containing compounds, such as ATP and GTP, stimulate the isomerase but have no influence on LRAT activity (15). In contrast, 11*c*ROL is a specific inhibitor of isomerase activity (16).

Protein interactions with RPE65 may also alter the isomerase activity. For example, RPE65 have been shown to interact with 11*c*RDH and the retinal G protein-coupled receptor RGR (8, 17). RGR belongs to the opsin family and participates in the regeneration of 11*c*RAL in the RPE (18). Using knock-out mice, RGR was shown to enhance the isomerase activity of RPE65 independently of light (19). Later, RGR was demonstrated to inhibit LRAT activities and to mediate light-dependent translocation of a*t*RE for synthesis of visual chromophore (20). These data established that RGR plays a regulatory role in the visual cycle.

Looking for potential protein partners of the isomerization process using a two-hybrid screening, we found that RPE65

* This work was supported in part by private foundations (Fédération des Aveugles et Handicapés Visuels de France, IRRP, Retina France, SOS Rétinite), Région Languedoc Roussillon, French Ministry for National Education, and Inserm.

[S] The on-line version of this article (available at http://www.jbc.org) contains supplemental Figs. S1 and S2.

[1] To whom correspondence should be addressed. Tel.: 33-499-636-052; Fax: 33-499-636-020; E-mail: philippe.brabet@inserm.fr.

[2] The abbreviations used are: 11*c*RAL, 11-*cis*-retinaldehyde; a*t*RAL, all-*trans*-retinaldehyde; atROL, all-*trans* retinol; 11*c*ROL, 11-*cis*-retinol; atRE, all-*trans* retinyl ester; atRP, all-*trans* retinyl palmitate; BCIP/NBT, 5-bromo-4-chloro-3-indolyl phosphate/nitro blue tetrazolium; CRALBP, cellular retinaldehyde-binding protein; EGFP, enhanced green fluorescent protein; FATP1, fatty acid transport protein 1; FATP1c, C-terminal 307 amino acid residues of FATP1; DBD, DNA binding domain; AD, transactivating domain; GST, glutathione *S*-transferase; LRAT, lecithin:retinol acyltransferase; RD, inherited retinal degeneration; 11*c*RDH, 11-*cis*-retinol dehydrogenase encoded by *RDH5* gene; RGR, retinal G protein-coupled receptor; RPE, retinal pigment epithelium; RPE65, RPE-specific 65-kDa protein; SLC27A1, solute carrier family 27 member 1; ER, endoplasmic reticulum.

interacts with the fatty acid transport protein 1, FATP1, also named SLC27A1, solute carrier family 27 (fatty acid transporter), member 1. Furthermore, we show that FATP1 reduces 11*c*ROL production in cellular models, affecting level of a*t*RE generated by LRAT activity and inhibiting isomerase activity without affecting level of RPE65 protein. These data raise the possibility that FATP1 alleles may modify RD phenotypes caused by defects in the visual cycle.

EXPERIMENTAL PROCEDURES

Materials—The full-length open reading frame of the human *RPE65* gene was kindly provided by Dr. Christian Salesse, and the Matchmaker™ library construction, and the screening kit as well as pGADT7-AD and pEGFP-C1, pECFP-N1, and pRK5 vectors were from BD Biosciences Clontech. Other materials are: remaining pCMV-epitope tag vectors (Stratagene, La Jolla, CA) and pFastBacDual (Invitrogen Corp., Carlsbad, CA), monoclonal mouse anti-RPE65 antibodies (clone 8B11.37 kindly provided by Dr. Debra Thompson and clone MAB5428, Chemicon, Temecula, CA), polyclonal rabbit (generous gift from Dr. Dean Bok) and monoclonal mouse (clone 1A11, Abnova, Taiwan) anti-LRAT antibodies, polyclonal rabbit anti-CRALBP antibody pAb UW55 (generous gift from Dr. John Saari), polyclonal rabbit anti-mouse FATP1 (generous gift from Dr. Jean Schaffer), monoclonal mouse anti-FLAG M2 antibody, alkaline phosphatase-conjugated IgG, and BCIP/NBT-purple liquid substrate (Sigma); horseradish peroxidase-conjugated IgG (Jackson ImmunoResearch Lab., West Grove, PA), glutathione-Sepharose beads, PVDF Hybond-P membranes, enhanced chemiluminescence Western blot-detecting reagents and the immunoprecipitation starter pack (Amersham Biosciences Europe, GmbH, Germany); BCA protein assay kit (Pierce); protease inhibitors mixture (Roche Diagnostics, Mannheim, Germany); Laemmli sample buffer (Bio-Rad); RNAxel kit (Eurobio, France); Oligotex kit (Qiagen); Superscript II reverse transcriptase (Invitrogen); Wizard SV gel kit; and Taq polymerase (Promega). All constructs and PCR products were sequenced using a BigDye Terminator Sequencing kit (Applied Biosystems, Foster City, CA) and an ABI 310 Prism automated sequencer (Applied Biosystems).

Two-hybrid Library and Bait Construction—The two-hybrid library was prepared using CDS III random-primer to prime poly(A)$^+$ RNA isolated from porcine RPE following the MATCHMAKER library construction and screening kit instructions. To use human RPE65 protein and fragments (see supplemental materials for construction) as baits, cDNA was ligated in-frame with GAL4 DNA binding domain into pGBKT7 DNA-BD cloning vector to transform the yeast reporter strain, AH109 (*Saccharomyces cerevisiae*). Human LRAT and tLRAT, which were also used as baits were cloned from retina and constructed according to Ref. (21), respectively.

Yeast Two-hybrid Analysis—The interaction between RPE65 and library-encoded proteins was phenotypically detectable on nutritionally deficient agar plates containing SD/Dropout (DO) medium, a combination of a Minimal SD Base combined and a DO supplement lacking leucine (LEU2 reporter gene), tryptophan (TRP1), adenine (ADE2), and histidine (HIS3) and with the secreted α-galactosidase activity (MEL1). Expression vector pGADT7-Rec containing RPE65-interacting proteins were isolated and the entire cDNA inserts were sequenced. *In silico* analysis was performed with in-frame sequences to identify genes. To eliminate false positives, relevant clones were tested again by co-transformation of AH109 yeast with either pGBKT7-RPE65 or pGBKT7-LamC or empty pGBKT7 vectors.

RNA Extraction and RT-PCR Expression Analysis—Porcine tissues were purchased from INRA Rennes (UMR SENAH, Saint-Gilles, France). Porcine retina and RPE were prepared as described below. Total RNAs were collected with RNAxel kit and mRNAs were then purified with Oligotex kit following manufacturer's instructions. 500 ng of each mRNA pool were reverse-transcribed in a 20-μl reaction mixture containing 250 ng of random primer and 200 units of Superscript II reverse transcriptase at 42 °C for 60 min. One microliter of the cDNA was then amplified in a 20-μl PCR using gene-specific primers and 2 units of Taq polymerase for 25–30 cycles. The 503-bp RPE65 product was amplified using the primers forward 5′-CTGCAGTGACCGATTCAAGCCATC-3′ and reverse 5′-CACTGCACAGAATTGCAGTGGCAG-3′; the 500-bp FATP1 product was amplified with the primers forward 5′-ATGCTGGACCTTCGCACAGCTGGA-3′ and reverse 5′AATGCGGTAGTACCTGCTGTGCAC-3′; the 300-bp GAPDH product was amplified with the primers forward 5′-CCCTGCAAATGAGCCCCAGCCTT-3′ and reverse 5′-TTGGTCGTATTGGGCGCCTGGTCA-3′. Buffer or genomic DNA contaminations were assessed in all assays by PCR without cDNA or reverse transcriptase. PCR products were analyzed in 2% ethidium bromide-agarose, then purified with a Wizard SV gel kit and sequenced.

GST Pull-down Assay—The FATP1c nucleotide sequence isolated from the two-hydrid contains the native TGA stop codon and untranslated sequence. The full-length was subcloned into pGEX-4T1 vector using EcoRI and XhoI restriction sites. To produce glutathione *S*-transferase (GST) and GST-FATP1c fusion proteins, *Escherichia coli* BL21 cells were transformed with pGEX-4T1 plasmids and growth at 30 °C for 3–4 h in 2*x*YT medium with 100 μg/ml ampicillin and 0.1 mM isopropyl-1-thio-β-D-galactopyranoside. Bacteria were sonicated 6 times for 15 s on ice in 1.5 ml BBIP buffer (phosphate-buffered saline with 5% glycerol, 5 mM $MgCl_2$, 0.1% Triton X-100, and protease inhibitor mixture). The extracts were incubated with 1% Triton X-100 for 1 h at 4 °C and centrifuged twice at 12,000 × *g* for 15 min. Aliquots of supernatants were incubated with 50 μl of glutathione-Sepharose beads for 1 h at 4 °C and washed twice with 200 μl of ice-cold BBIP with 150 mM NaCl to isolate GST proteins. RPE homogenate (1.3 mg/ml protein) was solubilized in BBIP supplemented with 0.5% Triton X-100 for 1 h at 4 °C and centrifuged at 20,000 × *g* for 20 min. 50 μg of RPE protein were incubated with GST alone or GST-FATP1c bound to glutathione-Sepharose beads overnight at 4 °C. Beads were washed five times with 200 μl of ice-cold BBIP-150 mM NaCl-0.1% Triton X-100 and resuspended in Laemmli sample buffer. An equal amount of bound proteins was separated in each lane by SDS-PAGE and analyzed by Western blot using anti-RPE65 (1:5,000) and anti-GST (1:100,000), then detected with horseradish peroxidase-conjugated IgG (1:10,000) and enhanced chemiluminescence reagents.

FATP1 Antibody and Western Blotting—A rabbit polyclonal FATP1 antibody was produced against GST-FATP1c purified on glutathione beads and dialyzed against phosphate-buffered saline. Antiserum was affinity-purified onto GST-FATP1c-glutathione-Sepharose column and used for Western blot analysis. Samples were solubilized in Laemmli sample buffer and ran in 10% SDS-PAGE. The proteins were transferred to polyvinylidene difluoride membranes, incubated overnight at 4 °C with specific primary antibodies (1:1,000), subjected to alkaline phosphatase-conjugated IgG (1:5,000) and revealed with BCIP/NBT-purple liquid substrate.

Expression of FATP1, RPE65, LRAT, and CRALBP in Sf9 Cells and Immunoprecipitation—Human FATP1, RPE65, LRAT, and CRALBP were cloned into pFastBacDual vector and recombinant bacmids were generated to produce high-titer baculoviruses stocks. *Sf9* cells were cotransfected with P2 stock of baculoviruses encoding FATP1 and RPE65/CRALBP.

For the immunoprecipitation assays, adherent cells were grown 3 days post-infection, and lysed into 50 mM Tris, pH 8.0 with protease inhibitor mixture and different detergent (IGEPAL CA-630, radioimmune precipitation assay buffer) and salt (0–150 mM NaCl) compositions to optimize the lysing conditions. Immunoprecipitation was performed according to instructions of the immunoprecipitation starter pack using antibodies against FATP1c and RPE65. The immune complexes were precipitated with protein G-Sepharose, washed several times and separated by SDS-PAGE, followed by Western blotting.

Porcine RPE Cell Isolation and Subcellular Fractionation—Fresh porcine eyes obtained from local slaughterhouse were opened on ice and the neuroretina removed from eyecups. The RPE was gently brushed and centrifuged for 15 min at 1170 × *g*. The pellet was resuspended in 150 mM NaCl, 10 mM Tris-HCl, pH 7.4, and homogenized in a Teflon-glass potter. Unbroken cells, nuclei, mitochondria, and heavy membranes were pelleted at 30,000 × *g* for 20 min. The supernatant was ultracentrifuged at 105,000 × *g* for 1 h to separate the cytosolic fraction from the pelleted microsomal fraction. The protein concentration was determined with a BCA protein assay kit. Similar subcellular fractionation was performed onto 293 and Sf9 cells.

Immunofluorescence Analysis of Cells and Retina—Human RPE65 cDNA was fused to N-terminal enhanced green fluorescent protein (EGFP) gene in pEGFP-C1 vector. EGFP-RPE65 was stably expressed into 293 cells (293-R) using Lipofectamine 2000 transfection method (Invitrogen) followed by Geneticin selection. In the meantime, 293 cells stably expressing ECFP-LRAT and EGFP-RPE65 (293-LR) were generated with the same method. GFP-positive cells were sorted by flow cytometry. A pCMV-FLAG-FATP1 (see supplemental materials for construction) was transiently transfected in 293-R cells using Lipofectamine 2000, according to the manufacturer's procedures. Cells were grown on FluoroDish (FD35–100, World Precision Instruments, UK) for an additional 24–48 h after transfection in Dulbecco's modified Eagle's medium with 10% heat-inactivated fetal bovine serum plus penicillin-streptomycin and fixed with 4% paraformaldehyde.

Immunocytochemistry was then performed according to Ref. 22 using anti-FLAG (1:1000). Confocal imaging was performed with a Zeiss LSM 5 LIVE DUO system. The image acquisition was obtained with the Zeiss LSM AIM software. For immunohistochemistry, C57BL/6J eyes were rapidly removed and fixed in 4% PFA, 24 h at 4 °C. Eyes cups were embedded in 5% low-melting agar and cut into 50-μm sagittal sections. Sections were permeabilized with 0.1% SDS, saturated 20 min with 10% fetal calf serum, and incubated overnight with the primary antibodies (rabbit anti-FATP1, 1/250; mouse anti-RPE65, 1/500). The secondary antibodies were diluted in phosphate-buffered saline (Alexa568-conjugated anti-rabbit, Alexa488-conjugated anti-mouse) and incubated 1 h. Sections were then mounted in Fluorsave™ Reagent (Calbiochem).

Isomerase and LRAT Assays in 293T, 293T-LC,293-LR, and Sf9 Cells—The 293T and 293T-LC cells stably expressing LRAT plus CRALBP (23) and the 293-LR were grown in Dulbecco's modified Eagle's medium supplemented with 10% heat-inactivated fetal bovine serum and penicillin-streptomycin at 37 °C under 5% CO_2. 293T and 293-LC cells were transfected using PolyFect reagent (Qiagen) and 293LR with Lipofectamine 2000, according to the manufacturer's procedures.

Isomerase Assay in Living Cells—This assay was done as described previously (23). Briefly, the 293T-LC cells transfected with expression vectors for RPE65 and FATP1 were incubated with 5 μM a*t*ROL in the medium for indicated times and lysed in 0.5 ml of 10 mM HEPES 0.2% SDS. During 293 cell transfection, pRK5 (empty expression vector) was added for single protein expression to normalize plasmid amount. Proteins (10 μg) were analyzed by immunoblot using RPE65 antiserum. Esters were saponified with 0.5 mM KOH at 55 °C for 15 min. Retinoids were extracted with hexane and analyzed by high performance liquid chromatography (HPLC). Identified peaks were confirmed by spectral analysis and coelution with authentic retinoid standards.

In Vitro Isomerase Assay—The *Sf9* cells were harvested at 2 days post-infection with baculoviruses expressing FATP1, RPE65, LRAT, and GFP (irrelevant protein), homogenized in 40 mM HEPES buffer (pH 7.5). The isomerase assay mixtures contained 20 mM HEPES, 100 mM NaCl, 6% bovine serum albumin, 10 μM all-*trans* retinyl palmitate (a*t*RP), 6.0 mM sodium cholate, and 1 mg of protein. After incubation for 30 min, 1 h, 1.5 h, and 2 h in the dark at 37 °C, the reactions were quenched by adding 0.2% SDS and 2 volumes of methanol. Retinoids were analyzed as described above.

LRAT Assay in Living Cells—293T cells in 12-well plates were transfected with pRK5 and LRAT or FATP1- and LRAT-expressing plasmids. At 36 h post-transfection, cell medium were replaced with fresh medium containing 5 μM a*t*ROL and incubated for 15 min, 30 min, and 1 h in the dark at 37 °C. 293-LR cells in 6-well plates were transfected with pRK5 or pCMV-FLAG-FATP1. At 36 h post-transfection, cell medium were replaced with fresh medium containing 10 μM a*t*ROL and incubated for 0.5, 1, 3, 6, and 18 h in the dark at 37 °C. After washing with phosphate-buffered saline, the cells were pelleted by low-speed centrifugation and lysed before retinoid analysis.

In Vitro LRAT Assay—The *Sf9* cells were harvested at 2–3 days post-infection with baculoviruses expressing FATP1 and/or LRAT, homogenized in 10 mM bis Tris propane-HCl buffer (pH 7.5), 100 mM NaCl. The LRAT assay mixtures con-

tained 10–20 μM a*t*ROL, 0.5% bovine serum albumin, and 200 μg of protein. After incubation for different times (as indicated) in the dark at 37 °C, the reaction was stopped, and retinoids were analyzed as described above.

RESULTS

Yeast Two-hybrid Screen and Identification of FATP1 as an RPE65-interacting Protein—From pig RPE we constructed yeast two-hybrid GAL4 AD/library, which was used to transform AH109 yeast expressing a GAL4 DNA-BD/human RPE65 fusion protein. GAL4 DNA-BD/RPE65 alone failed to activate transcription of the HIS3 and LacZ reporter genes, indicating that RPE65 does not function as a transcriptional activator and can be used as bait (data not shown). A total of 1.2×10^6 individual clones were screened by growth selection of yeast colonies. Among these, 112 positives clones were identified. Additional controls and sequence analysis allowed us to further identify 12 (11%) true positive clones. One of these clones contained a cDNA encoding part (the C-terminal 307 amino acids) of porcine FATP1, known to play a role in fatty acid metabolism. The 307-amino acid fragment (herein referred to as FATP1c) is highly conserved among mammalian species and notably shows 95% identity with its human ortholog (supplemental Fig. S1*A*). Importantly, based on the proposed membrane topology model of FATP1 by Lewis *et al.* (24), the main part of FATP1c projects into the cytosol while its N-terminal part is embedded in the lipid bilayer membrane (supplemental Fig. S1*B*).

Characterization of FATP1c Interactions in Yeast—Transformed yeast failed to grow when FATP1c was paired with lamin C (Fig. 1*A*, sector 10), indicating that FATP1c alone was unable to activate transcription. In contrast, yeast grew when co-transformed with FATP1c and with human full-length RPE65 (Fig. 1*A*, sectors 2 and 9) or with truncated RPE65 fragments: RPE65/N147 (amino acids 1–147; sector 6); RPE65/140–318 (amino acids 140–318, sector 7), and RPE65/311C (amino acids 311–533; sector 8). Conversely, FATP1c interacted with tLRAT, a LRAT deleted of the putative N- and C-transmembrane termini (Fig. 1*A*, sector 3), but not with the full-length LRAT (Fig. 1*A*, sector 4), demonstrating that the LRAT transmembrane domains were incompatible with the yeast two-hybrid assay.

We evaluated the strength of these interactions by assessing yeast densities from colonies expressing the Ade+/His+/Leu+/Trp+ phenotype grown to mid-log phase (Fig. 2*B*). The truncated RPE65 fragments and tLRAT showed a significantly stronger interaction than full-length RPE65. Interestingly, yeast transformed with RPE65-N147 grew significantly faster (up to 50% increase) than those expressing other fragments and reached at least 80% of the standard value, suggesting that the N terminus of RPE65 was sufficient to achieve the highest interaction. In any case, yeast growth differences were not consistent with expression variability among the polypeptides (Fig. 2*C*).

Isolation of FATP1-RPE65/LRAT Protein Complexes—To confirm these interactions, a GST-FATP1c fusion protein purified with glutathione-Sepharose beads was incubated with detergent-solubilized porcine RPE proteins (Fig. 2*A*). The native porcine RPE65 was retained in a dose-dependent manner by GST-FATP1c but not by the GST protein regardless of concentration. However, we could not attribute any relative affinity for RPE65 because the GST fusion protein showed variable binding efficiencies that remained low when compared with input RPE65 signal. We then evaluated recombinant protein interaction by co-immunoprecipitation (Co-IP) experiments carried out with *Sf9* cells co-expressing human FATP1, RPE65, LRAT, and CRALBP (Fig. 2*B*). Using increasing amounts of anti-FATP1, FATP1 co-precipitated with both RPE65 and LRAT but not with CRALBP. The reverse Co-IP with anti-RPE65 demonstrated that both FATP1 and CRALBP specifically interact with RPE65 but that LRAT did not. We concluded that FATP1 does biologically interact with RPE65 and LRAT, and that these interactions are independent of each other.

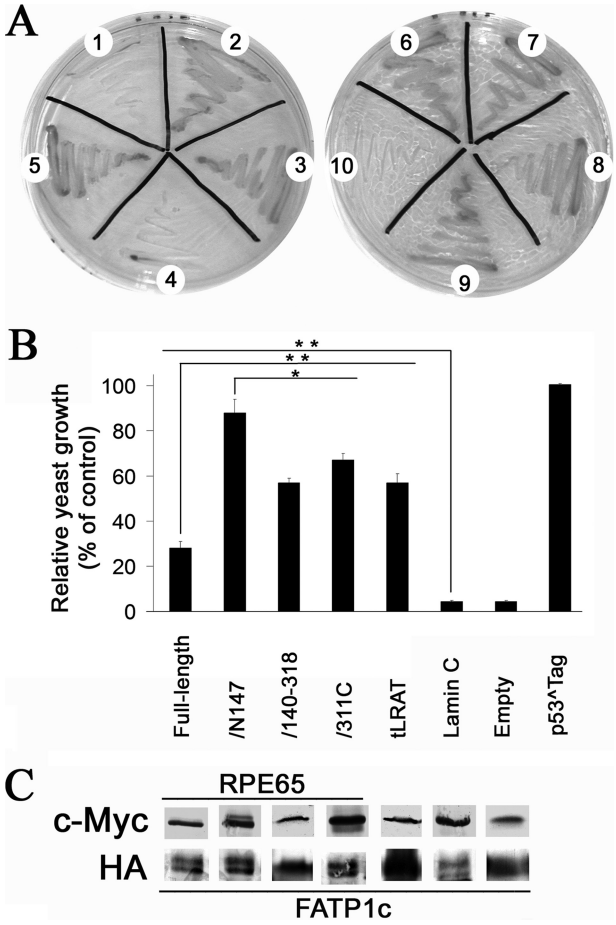

FIGURE 1. **RPE65-FATP1c interaction in yeast two-hybrid assays.** *A*, specificity of FATP1c interaction with RPE65 and tLRAT. Yeast co-transformed with GAL4BD-full-length RPE65 (sector 2 and 9, RPE65), amino acids 1–147 (sector 6, RPE65-N147), 140–318 (sector 7, RPE65/140–318), 311–533 (sector 8, RPE65/311C), and GAL4AD-FATP1c grew on SD/-Leu/-Trp/-His/-Ade/+X-α-gal. Co-transformants with GAL4BD (sector 1, Empty) or GAL4BD-LaminC (sector 10, Lamin C) and GAL4AD-FATP1c did not grow (nonspecific interaction control). Transformants with GAL4AD-tLRAT (sector 3, tLRAT) + GAL4BD-FATP1c grew but not with GAL4AD-LRAT (sector 4, LRAT) + GAL4BD-FATP1c. Co-transformation with GAL4BD-p53 and GAL4AD-Tag (sector 5, p53^Tag control) served as a positive reference. *B*, relative strength of protein interactions. Individual transformed yeasts were grown at 30 °C until the mid-log phase. Relative yeast growth was expressed as an A_{600} ratio of sample to p53^Tag control. Histogram values are means ± S.D. (n = 3–7 in triplicates). *, $p < 0.01$; **, $p < 0.001$ (Student's t test). *C*, expression of hybrid proteins in co-transformed yeast. Western blot experiments performed on yeast extracts with anti-c-Myc (bait vectors) and anti-HA (prey vectors) antibodies.

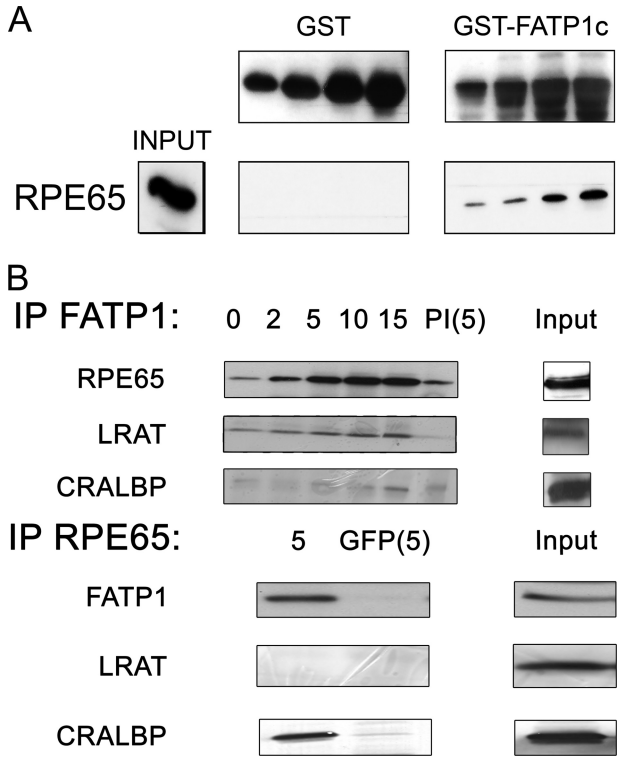

FIGURE 2. **Interactions between FATP1, RPE65, and LRAT.** *A*, representative GST pull-down assay ($n = 3$). 0.5, 1.5, 3, 5 μl of GST and 10, 30, 60, 100 μl of GST-FATP1c were evaluated on Western blot with anti-GST antibody (*upper panels*) and used in pull-down with 50 μg of RPE protein, RPE65 was blotted with anti-RPE65 (1:1,000), and detected with ECL. A fifth of the input identified RPE65 in RPE lysates before pull-down. *B*, co-immunoprecipitation assay. *Sf9* cells were lysed and incubated with anti-FATP1 (*IP FATP1*) or -RPE65 (*IP RPE65*) antibodies. Immune complexes were precipitated and analyzed by Western blotting. 2–15 μl of FATP1 antibody were used for IP FATP1. 5 μl of rabbit pre-immune (*PI*) served as control. 5 μl of RPE65 or GFP (*control*) antibody was used in IP RPE65 assays. Inputs were 1:10–20 of IP volumes.

FATP1 Expression and Co-localization with RPE65 in the Retinal Pigment Epithelium—We first examined the distribution of FATP1 in pig tissues by semi-quantitative RT-PCR using tissue-specific poly(A)+ RNA. *FATP1* transcripts were detected in various tissues (Fig. 3*A*). The highest expression level was found in the RPE (strong and specific *RPE65* expression served as a control). High levels were also found in heart, brain, and skeletal muscle whereas lung, kidney, liver, and skin showed lower levels. No expression was detected in intestine and thymus. FATP1 transcripts were also detectable in both neural retina and RPE (data not shown).

The protein expression analysis by immunoblotting with the FATP1c antibody showed an immunoreactivity at 63 kDa in tissues where FATP1 is known to be well expressed, such as white adipose tissue, skeletal muscle, and heart. The immunoreactivity was lower in liver and absent in intestine. An immunoreactive band was also detected in RPE/retina (Fig. 3*B*).

We further investigated the FATP1 subcellular distribution in porcine RPE cells. Separation of membranes into pellet (P; nucleus, mitochondria, lysosomes, cytoskeleton), microsomes (M; ER and plasma membrane) and cytosol (C) by differential centrifugations and subsequent Western blotting demonstrated the presence of a 63-kDa FATP1 band that, like RPE65 and LRAT, was localized in microsomes (Fig. 3*C*). Weak FATP1

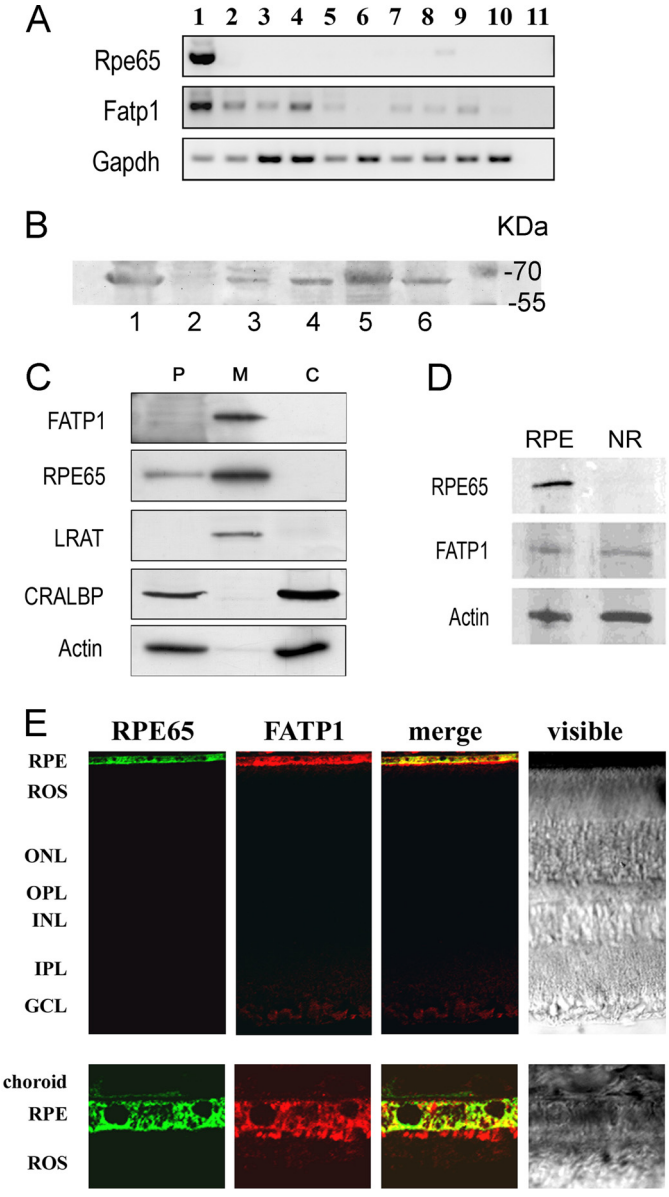

FIGURE 3. **Cellular and tissular co-localization of FATP1 and RPE65.** *A*, expression of porcine FATP1 and RPE65 mRNA. Representative RT-PCR ($n = 3$) were performed on pig mRNA from tissues: *1*, RPE; *2*, brain; *3*, skeletal muscle; *4*, heart; *5*, liver; *6*, intestine; *7*, skin; *8*, lung; *9*, kidney; *10*, thymus, *11*, negative control without RT. *B*, porcine tissue survey immunoblot on 100 μg proteins with the anti-FATP1c antibody including RPE/retina (1), intestine (2), liver (3), heart (4), skeletal muscle (5), and white adipose tissue (6). *C*, FATP and isomerase-processing components in RPE subfractions. Pig RPE cells were fractionated by gradient density centrifugation into 30,000 $\times$ *g* pellet (*P*), microsomal (*M*), and cytosolic (*C*) fractions. Western blot analyses were performed on 50 μg of proteins from P and C, 5 μg from M with various antibodies against FATP1, RPE65, LRAT, CRALBP, and actin. *D*, Western blot analysis of RPE65, FATP1, and actin in mouse RPE and neural retina (*NR*). *E*, immunohistolocalization of RPE65 and FATP1 in RPE/retina vibratome sections. Differential interference contrast image of mouse retina shows RPE, rod outer segment (*ROS*), outer (*ONL*, *OPL*), and inner (*INL*, *IPL*) nuclear and plexiform layers, and ganglion cell layer (*GCL*). FATP1 immunolabeling (*red*) was restricted to RPE and GCL, whereas RPE65 (*green*) was confined to RPE. Higher magnification focuses on the RPE.

and RPE65 bands were also detected in the P fraction (30,000 $\times$ *g* pellet). In contrast, CRALBP was found in the C and P fractions.

Lastly, Fatp1 expression was studied in the mouse retina using an antiserum against residues 628–640 of the murine

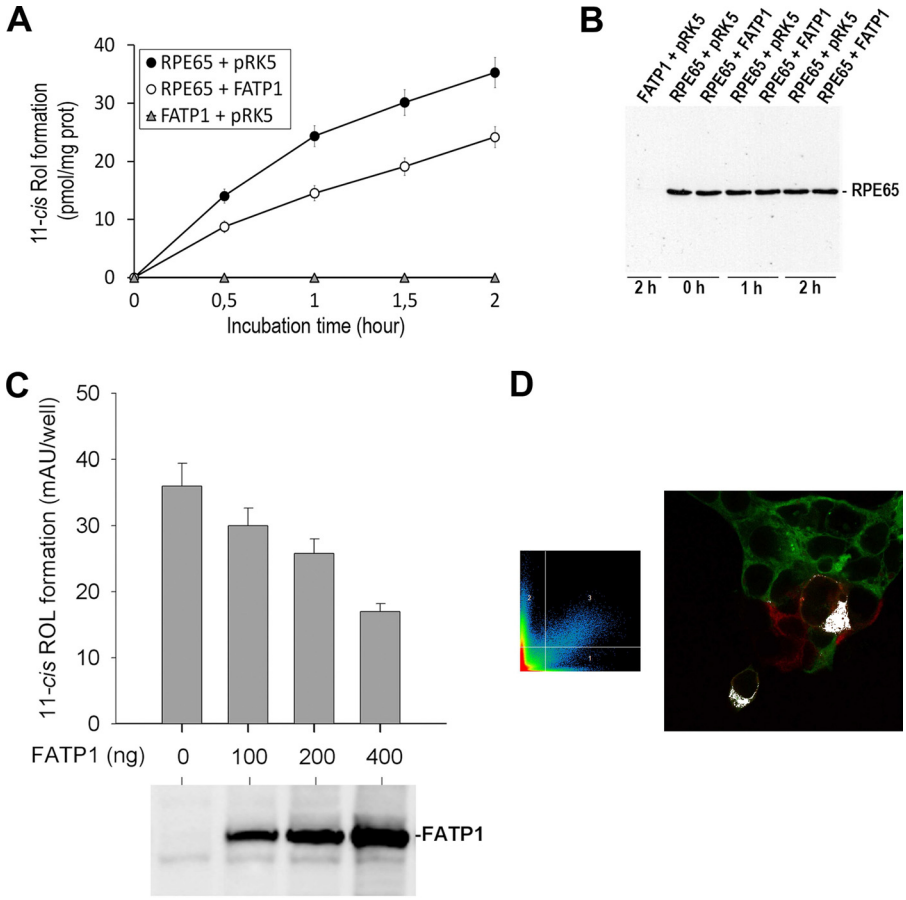

FIGURE 4. **FATP1 inhibits 11-*cis* retinol formation.** RPE65 or FATP1 or RPE65 plus FATP1 were transiently expressed in 293T-LC (*A–C*) cells. Following addition of 5 μM a*t*ROL in the culture medium, 11*c*ROL formation was measured after different incubation times (*A*) or after 3 h in dark following co-transfection of RPE65 with various amount of FATP1-expressing plasmid (*C*) as indicated. Values were expressed as pmol/mg protein (mean ± S.D., $n \geq 3$). *B*, immunoblot analysis of RPE65 expression in transfected cells. *D*, RPE65 and FATP1 localization by confocal imaging. 293-R cells expressing GFP-RPE65 (*green*) were transfected with a FLAG-FATP1 expressing plasmid and labeled with the anti-FLAG (*red*). Z stacks were projected into one slice and a scatter diagram (*left panel*) based on intensity thresholds defining channel 1 (*GFP*), channel 2 (*rhodamin*), background (*horizontal* and *vertical lines*), and colocalization region (3). *Right panel* shows the combined image with mask overlay in *white*.

Fatp1 sequence. This antibody recognized a 63-kDa band in both RPE and neuroretina by Western blotting (Fig. 3*D*). As shown in Fig. 3*E*, Fatp1 was observed mainly in the RPE monolayer, and at a lower level in the ganglion cell layer, but nowhere else in the neuroretina. In the RPE, Fatp1 co-localized with RPE65 except in the apical microvilli where only Fatp1 immunoreactivity was detected.

FATP1 Inhibits RPE65-mediated 11-cis Retinol Production—We evaluated the impact of FATP1 on the RPE65 and LRAT activities. 293T cells stably expressing LRAT and CRALBP (293T-LC) were transiently transfected with plasmids highly expressing RPE65 or FATP1 alone or RPE65 plus FATP1. Following addition of 5 μM a*t*ROL to the culture medium, the synthesis of 11*c*ROL was measured over the time (Fig. 4*A*). In the presence of RPE65, 11*c*ROL was detectable as early as 30 min after addition of a*t*ROL and increased within the next 2 h. In contrast, the cells which only expressed FATP1 did not show any isomerase activity. When RPE65 and FATP1 were co-expressed, the formation of 11*c*ROL was lower at each time point. Importantly, the expression levels of RPE65 in all conditions were similar (Fig. 4*B*), indicating that the decreased isomerase activity in the cells transfected with RPE65 plus FATP1 was not due to altered expression levels of RPE65. Because FATP1 interacts dose-dependently with RPE65 in protein-protein interaction assays, we looked for a dose-dependent effect on RPE65 isomerase activity. Fig. 4*C* clearly demonstrated that the level of inhibition depends on the FATP1 expression in the 293T-LC. Finally, to prove the co-localization of FATP1 with RPE65 in 293 cells, we stably expressed an EGFP-tagged human RPE65 in 293 cells and transiently transfected a FLAG-tagged human FATP1. We detected green fluorescent with a punctuated distribution in the cytoplasm that superimposed with an ERtracker (data not shown). In some cells, we revealed FATP1 expression with an anti-FLAG antibody (red fluorescence) and in a few of them, the confocal analysis demonstrated a perfect co-localization of FATP1- and RPE65-tagged proteins (*white merge*, Fig. 4*D*).

The decrease of the 11-*cis* production could result from an action of FATP1 on LRAT or RPE65 or both. To demonstrate a direct inhibition of RPE65, homogenates prepared from baculovirus-infected *Sf9* cells that expressed RPE65, FATP1, or both were incubated with a*t*RP, the isomerase substrate (Fig. 5*A*). The kinetics of 11*c*ROL production in *Sf9* was similar to that of 293T-LC: FATP1 markedly inhibited the synthesis of 11*c*ROL from a*t*RP in the presence of RPE65, the expression of which remained unchanged (Fig. 5*B*). In addition, we checked that RPE65 and FATP1 co-localized in the same membrane fraction from co-infection of *Sf9* cells (Fig. 5*C*). Therefore, we concluded that FATP1 directly inhibits the isomerase activity of RPE65.

FATP1 Decreases atRE Production—To measure LRAT activity, a*t*RE production was followed in 293T-LC cells during 1 h of *at*ROL incubation. Under this condition, FATP1 expression did not affect a*t*RE production (Fig. 6*A*). The next experiment was designed in 293 cells stably expressing LRAT and RPE65 (293-LR) incubated with 4 nmol a*t*ROL and a*t*ROL and a*t*RP were monitored for 18 h to allow the reaction to reach a plateau. The results of the experiment, shown in Fig. 6*B*, demonstrate that a*t*ROL is rapidly esterified within the first hour but reached at steady-state phase after 6 h at a value close to the accumulation of a*t*RP, a characteristic of a reaction at equilibrium. In the presence of FATP1, the cellular uptake of a*t*ROL was increased but the amount of a*t*RP produced was decreased

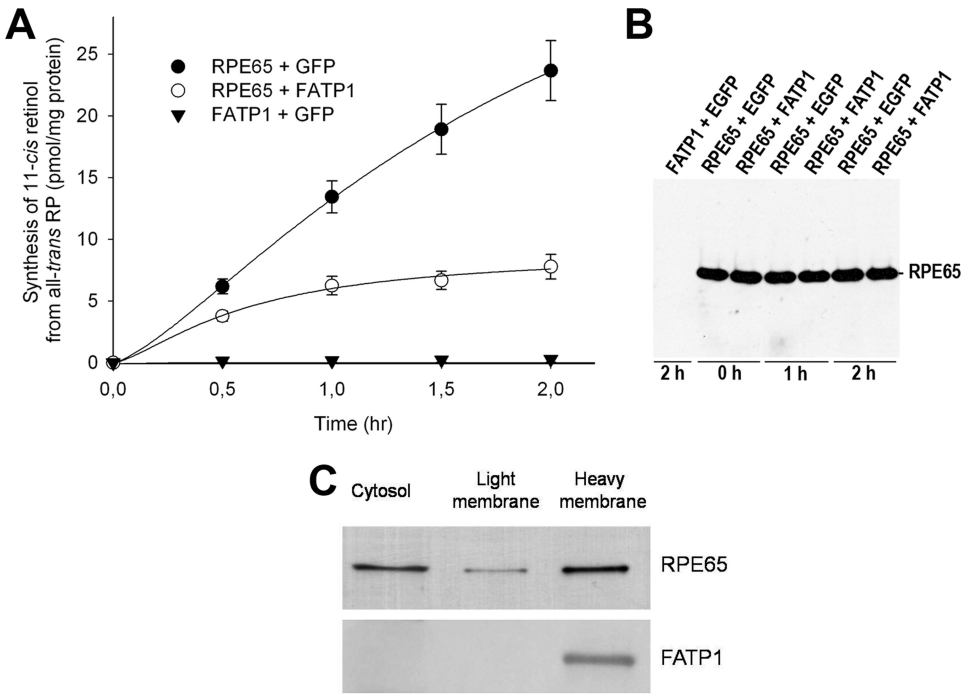

FIGURE 5. **FATP1 inhibits RPE65 isomerase activity.** Homogenates from Sf9 cells expressing RPE65 plus GFP, FATP1 plus GFP or RPE65 plus FATP1 were incubated with 10 μM a*t*RP for the indicated time, and retinoids were extracted. *A*, kinetics of 11*c*ROL formation. Values were expressed as pmol/mg protein (mean ± S.D., $n = 3$). *B*, immunoblot analysis of RPE65 expression during the reaction time. *C*, immunoblot analysis of RPE65 and FATP1 in subcellular fractions from Sf9 homogenate: cytosol, light membrane (30,000 × *g* pellet), heavy membrane (105,000 × *g* pellet).

after 3 h of incubation. Thus, it is apparent that FATP1 does not affect the initial activity of LRAT but enhances the transition to the steady-state condition in which the amount of a*t*RP does not appear to change.

To confirm this finding, *Sf9* cells were also used to express LRAT, FATP1, or both. In the presence of LRAT, the addition of a*t*ROL resulted in the production of retinyl esters. The amount of esters formed after 1 h of incubation decreases slowly with decreasing the level of LRAT present in this experiment (Fig. 7*A*). The kinetics of accumulation of retinyl esters showed that at high level of LRAT, the a*t*ROL was very quickly and fully converted into retinyl esters (Fig. 7*B*). In contrast, with a much lower level of LRAT (L/5), the synthesis of retinyl ester reached a plateau at 30 min of reaction, and all a*t*ROL was not esterified. As shown in Fig. 7*C*, co-expression of FATP1 under similar conditions did not alter the rate of retinyl ester synthesis at a high level of LRAT but significantly decreased this rate (16.5 ± 2.1%) after 30 min of reaction when the level of LRAT is reduced by four. Co-expression of FATP1 itself did not affect the expression of LRAT (Fig. 7*D*). Finally, we asked whether the substrates of FATP1, the palmitate, CoA, and ATP could modify the observed effect on the synthesis of retinyl esters. In the series of experiments, the dampening effect of FATP1 was very marked (60.6 ± 5.8% reduction). In these conditions, the substrates did not alter the activity of LRAT (Fig. 7*E*). As for RPE65, we verified that LRAT was localized with FATP1 in the same membranes (Fig. 7*F*). In conclusion, these data demonstrated that FATP1 inhibits the 11*c*ROL formation by interacting with both RPE65 and LRAT proteins and altering their functions.

DISCUSSION

RPE65, responsible for severe early-onset congenital blindness (25, 26), is the key-enzyme for regeneration of 11-*cis* conformation of vitamin A. The molecular mechanisms regulating this rate-limiting step are not yet fully known and could explain phenotypic variability in RD caused by analogous gene mutations (27). Our work has consisted of identifying, through yeast two-hybrid screening, new RPE65 protein partners, studying their modality of interaction with RPE65 and defining their regulatory role in the visual cycle. We demonstrated that FATP1 is a regulatory partner of both LRAT and RPE65 in the microsomal membrane of RPE cells.

Given that no structural information was available to delineate interacting domains, we used the full-length RPE65 open reading frame as bait in the two-hybrid screen. To analyze specific protein-protein interactions, we selected three RPE65 fragments, N147, 140–318 and 311C. The N-terminal 147 residues showed the highest interaction of the three fragments, suggesting that preferential FATP1 interaction may biologically occur within the N terminus of RPE65. Interestingly, the crystal structure of native RPE65 recently described shows that its N-terminal region could be available for interacting proteins (supplemental Fig. S2 and Ref. 28).

FATP1 was first identified in a functional screen for adipocyte proteins that facilitate fatty acid uptake into 3T3-L1cells (29). Later, FATP1 function was redefined as an acyl-CoA synthetase with broad specificity for both long (palmitate) and very long chain fatty acids (30, 31). FATP1 belongs to a large evolutionarily conserved family of integral membrane proteins with a molecular weight of 63 kDa. To date, five members have been described in mice and six in humans (FATP 1–5/6) (32), which show tissue-specific expression patterns. Here, we characterized the expression pattern of porcine FATP1 by the simultaneous analysis of mRNA and protein. The higher expression observed in skeletal muscle, heart, white adipose tissue, brain, and skin is consistent with that previously reported in mouse and human (29, 32–34). Moreover, we show for the first time that the RPE and retina also contains high levels of FATP1 expression.

Lewis *et al.* (24) depicted FATP1 as an integral membrane protein composed of one transmembrane domain near the N terminus of the protein; the N terminus faces the extracellular/luminal space, whereas the C terminus projects into the cytosol. In light of our observations, FATP1 interacts with the visual cycle proteins LRAT and RPE65 via its cytosolic domain, con-

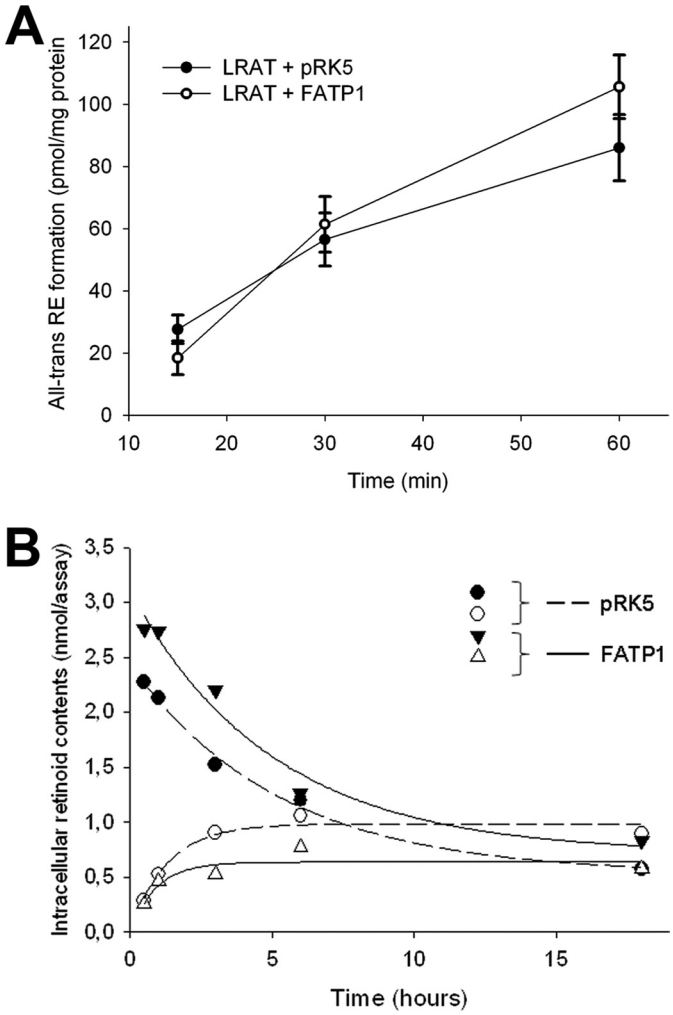

FIGURE 6. **FATP1 affects LRAT activity.** *A*, LRAT or LRAT plus FATP1 were expressed in 293T cells. Following addition 10 μM *at*ROL, synthesis of *at*RE was measured after different incubation times as indicated (mean ± S.D., $n \geq 3$). *B*, 293-LR cells were transfected with pCMV-FLAG-FATP1 or pRK5 vectors in 6 well plates and incubated with 10 μM *at*ROL for the time indicated and both *at*ROL and *at*RP were monitored. Values were expressed as nmol/well and were representative of two experiments.

sistent with its established membrane topology. Note that the two-hybrid system in yeast identifies only areas of interaction outside of the membrane bilayer. This has also forced to truncate the transmembrane domains of LRAT to study its interaction with FATP1. The FLAG-FATP expressed in 293-LR cells mainly localized in a cytoplasm network with a reticular pattern and superimposes with EGFP-RPE65 fluorescence, suggesting a correct targeting to the ER membrane. Moreover, after subcellular fractionation, FATP1 appears confined to RPE microsomes like RPE65 and LRAT. All together, our present results show that FATP1 functions mainly at the ER membrane. The proposal that FATP1 may not function as a plasma membrane fatty acid transporter was originally made after *in vitro* expression of functional tagged FATP1 proteins in intracellular membranes thus resulting in its characterization as a long-chain fatty acyl-CoA synthetase (24, 30). The acyl-CoA synthetase catalyzes esterification of long-chain fatty acids (LCFAs) with coenzyme A (CoA) and ATP as essential cofactors, the initial step required for all cellular LCFA utilization. This enzyme was indeed identified in the microsomal fraction and there was no evidence for acylation by the plasma membrane (35). Moreover, recent data obtained in cultured human myotubes suggested that FATP1 may function within an intracellular protein complex (36). FATP1 enhanced fatty acid import to this protein complex, trapping fatty acids and facilitating their access to other enzymatic pathways. Similar data were obtained with FATP4, that shares 62.5% aa identity with FATP1, and which has an acyl-CoA-synthetase activity and is in fact localized to the ER membrane (37).

Our data show that both LRAT and RPE65 co-localize in the microsomal fraction of porcine RPE cells but suggest that they do not form protein complexes. Indeed, no direct protein-protein interaction was seen using both two-hybrid and co-immunoprecipitation assays. These results are in agreement with the recent finding that LRAT is not an acyl-transferase for RPE65 and does not modify its membrane association and isomerase activity, but only serves to provide a*t*RE (6). In contrast, FATP1 interacts both with LRAT and RPE65 but does not link them together, suggesting that it may regulate their activities independently.

FATP1 markedly decreased the isomerase activity of RPE65 throughout the kinetics of 11*c*ROL production without affecting its expression levels, suggesting a direct enzymatic regulation. The mechanism of this regulation is not clear at present. It may be the result of subtle changes at the level of substrate binding or by an allosteric effect. The fact that RPE65-mediated isomerization is a limiting step of the visual cycle raises the intriguing question of the biochemical significance of this FATP1-inhibiting effect. This inhibition might be either transient (strong interaction) or constitutive (stable interaction) and thus participate in the apparent low isomerase activity of RPE65 (23). However, FATP1 appeared less abundant than RPE65 in the RPE and consequently its inhibitory effect on isomerase activity might involve a mechanism of negative cooperativity, FATP1 acting as a heterotropic modulator. Even if we do not provide evidence that the protein interaction is sufficient for inhibition, this is strongly suggested by the dose-dependence of both protein-protein interaction and isomerase inhibition. In addition, we propose that FATP1 acts on the isomerase activity rather than hindering the access of the substrate to RPE65 catalytic site because: 1) FATP1 interacts with RPE65 via extramembrane domains, whereas access of substrate to RPE65 is likely within the hydrophobic core of the ER membrane (17), and 2) isomerase inhibition is important in the homogenate from Sf9 cells under saturating substrate concentrations.

This study has also demonstrated that CRALBP forms complexes with RPE65. The absence of interaction between FATP1 and CRALBP supports the specificity of the FATP1 interaction with RPE65 and LRAT. CRALBP is an acceptor of 11-*cis* retinol that promotes retinoid isomerization. A high affinity binding site for 11*c*ROL appeared sufficient to drive isomerization by mass action, 11*c*ROL being selectively removed and oxidized to 11*c*RAL by 11*c*RDH (9, 10). Therefore, FATP1 and CRALBP probably exert opposite effects by different molecular mechanisms of regulation of RPE65 activity.

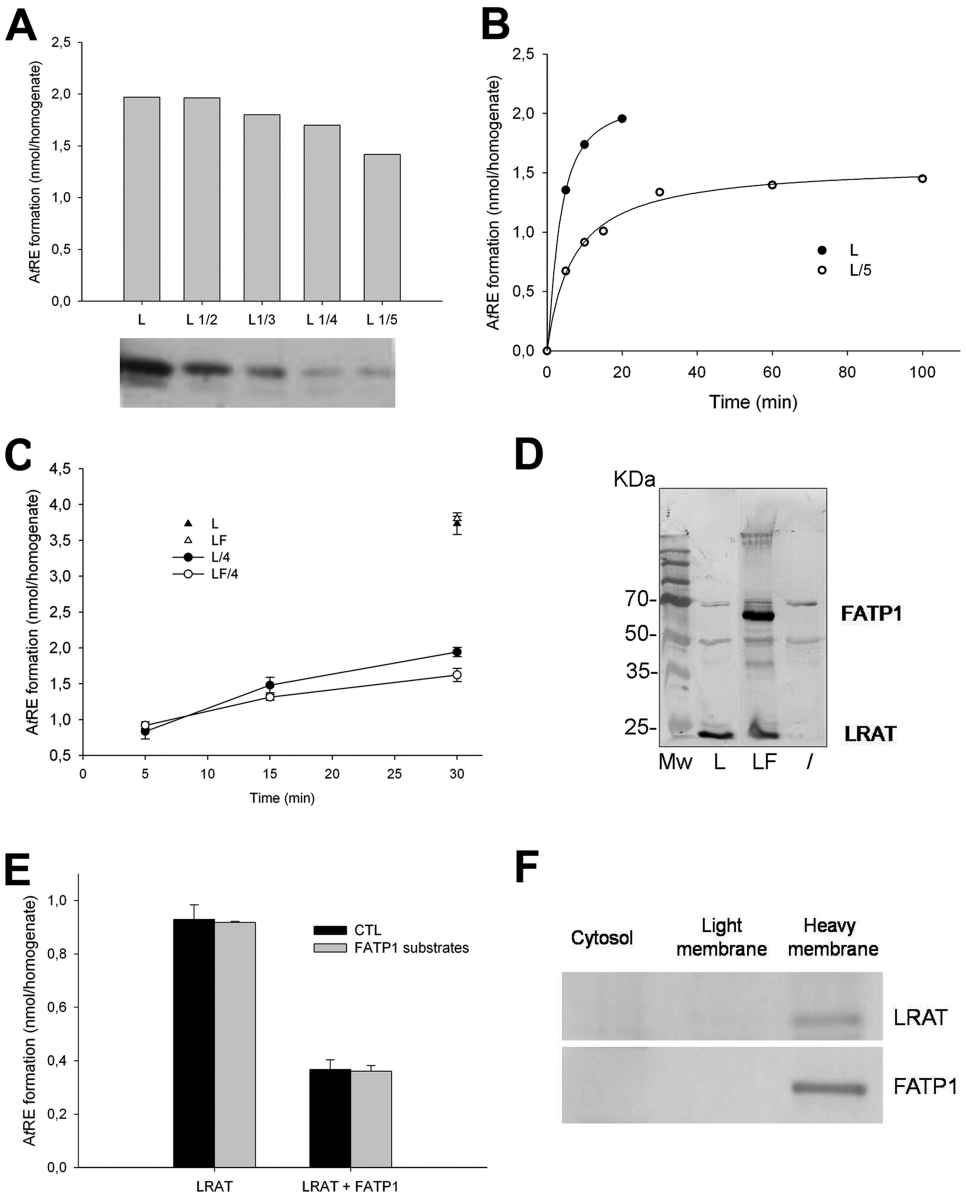

FIGURE 7. **FATP1 alters the balance of at*RE* synthesis.** *A*, levels of at*RE* in Sf9 cells infected with dilutions of LRAT-expressing baculovirus (L to L/5) and incubated with 10 μM at*ROL* for 1 h. Immunoblot analysis of LRAT expression is shown underneath. *B*, levels of at*RE* in Sf9 cells infected with two dilutions of LRAT-expressing baculovirus (*L* and *L/5*) and incubated with 5 μM at*ROL* for the indicated time. Data were represented as nmol/homogenate and were representative of two determinations. *C*, two dilutions of Sf9 cell homogenates expressing LRAT (*L* and *L/4*) or LRAT plus FATP1 (*LF* and *LF/4*) were incubated with 20 μM at*ROL* and at*RE* formation was monitored over time ($n = 3$). *D*, immunoblot analysis of FATP1 and LRAT expression in Sf9 cells used in *C*. *E*, levels of at*RE* in Sf9 cells expressing LRAT (*L*) or LRAT plus FATP1 (*LF*) incubated for 1 h with 10 μM at*ROL* and FATP1 substrates, 20 μM palmitate, 200 μM CoA, and 10 mM ATP ($n = 3$). *F*, immunoblot analysis of LRAT and FATP1 in subcellular fractions from Sf9 homogenate as in Fig. 5.

FATP1 did not affect the initial activity of LRAT, suggesting that protein interaction does not directly affect the acyltransferase. In RPE cells, LRAT catalyzes a CoA-independent esterification of at*ROL*, which results in a rapid burst of retinyl ester synthesis, followed by a plateau where the amount of retinyl ester does not change (38). Similar curves were observed in the present study within 293-LR and *Sf9* cells expressing adequate low level of LRAT activity under saturating at*ROL* concentrations. Saari *et al.* (39) have previously demonstrated that the reversibility of LRAT may contribute to the depletion of at*RE*. Moreover, the co-expression of FATP1 and LRAT in both cell lines resulted in significant decreases in the level of at*RE* production when the LRAT reaction has reached equilibrium. Therefore, one explanation could be that FATP1 stimulates the reversal of LRAT. Because FATP1 can mobilize palmitate as a substrate to produce palmitoyl-CoA, we would expect that it participates in a palmitate exchange in the LRAT reaction. However, addition of the substrates for FATP1 did modify neither the LRAT reaction nor the regulation by FATP1, suggesting that the acyl-CoA synthetase activity has no direct effect on the LRAT activities. This can be explained in part since the retinyl esters are synthesized by LRAT in a CoA-independent reaction (38). For the reversal of the LRAT reaction, it is unclear whether palmitate generated *in situ* by LRAT is equivalent to palmitate added to homogenates with respect to accessibility to the acyl-CoA synthetase. Further studies are needed to determine whether the acyl-CoA synthetase activity of FATP1 may be crucial for the reversal of the LRAT reaction.

The observations reported in this work suggest that FATP1 could operate on both LRAT and RPE65, a feature that may have physiological significance for the mobilization of at*ROL* pools. Light exposure of photoreceptor cells results in the release of at*ROL*, which may be taken up by RPE and esterified by LRAT (1). FATP1 may regulate the synthesis of at*RE* by acting on the reverse activity of LRAT, which functions as a retinyl ester hydrolase. Therefore, in response to light, FATP1 could limit the production of at*RE* in RPE while in darkness it might inhibit the production of 11*c*ROL acting on RPE65. As another example of regulation of the visual cycle in RPE, RGR was shown to both inhibits LRAT activities and enhances isomerase activity in darkness (19, 20). The explanation given by Radu *et al.* (20) is that activation of RGR by light stimulate LRAT and REH activities and the processing of at*RE* between lipid droplets and ER membranes where it can be converted to 11cROL by RPE65 in darkness. Accordingly, FATP1 and RGR could act on the synthesis of visual chromophore in regulating both LRAT and RPE65 in a light-dependent manner.

Defects in nearly every step of the visual cycle are responsible for RD (3). Retinitis pigmentosa (RP) and Leber congenital amaurosis (LCA) involve the impaired synthesis of visual chromophore leading to the degeneration of photoreceptor cells and are partly caused by loss-of-function alleles in RPE65 and LRAT (2). Macular dystrophy involves the accumulation of toxic lipofuscin fluorophores such as A2E derived from a*t*RAL in the RPE, which ultimately degenerate and cause photoreceptor cell death (3). As FATP1 inhibits the production of 11*c*ROL, a gain-of-function mutation in *FATP1* would potentially be deleterious in RP and LCA by phenotypic convergence. In contrast, it might have an important protective role in Stargardt disease by limiting the accumulation of a*t*RAL and A2E. Further *in vivo* experiments will be necessary to validate this assumption.

A growing number of reports provide evidence of multifaceted roles of energetic metabolism proteins (40). By its acyl-CoA synthetase activity, FATP1 activates fatty acids as the first step of many kinds of metabolism in different cell types. Our data demonstrate that in RPE cells, the targeting of FATP1 to the ER membrane may indicate a specific requirement for the metabolic retinoid cycle. This study provides new perspectives on the involvement of non-retinoid metabolism-related proteins in the regulation of the visual cycle.

Acknowledgments—We thank Drs. Debra A. Thompson, Dean Bok, John C. Saari, and Jean Schaffer for providing antibodies and Cécile Jolly and Yvan Boublik for the production of recombinant proteins and FATP1 antibodies. We would like to thank Audrey Weber, Bronia Ayoub, and Vaïmiti Revol for technical support, Chantal Ripoll and Hassan Boukhaddaoui for a plateform services, and Vasiliki Kalatzis for critical reading of the manuscript.

REFERENCES

1. Rando, R. R. (2001) *Chem. Rev.* **101,** 1881–1896
2. Thompson, D. A., and Gal, A. (2003) *Prog. Retin. Eye Res.* **22,** 683–703
3. Travis, G. H., Golczak, M., Moise, A. R., and Palczewski, K. (2007) *Annu. Rev. Pharmacol. Toxicol.* **47,** 469–512
4. Mondal, M. S., Ruiz, A., Hu, J., Bok, D., and Rando, R. R. (2001) *FEBS Lett.* **489,** 14–18
5. Xue, L., Jahng, W. J., Gollapalli, D., and Rando, R. R. (2006) *Biochemistry* **45,** 10710–10718
6. Jin, M., Yuan, Q., Li, S., and Travis, G. H. (2007) *J. Biol. Chem.* **282,** 20915–20924
7. Moiseyev, G., Chen, Y., Takahashi, Y., Wu, B. X., and Ma, J. X. (2005) *Proc. Natl. Acad. Sci. U.S.A.* **102,** 12413–12418
8. Simon, A., Hellman, U., Wernstedt, C., and Eriksson, U. (1995) *J. Biol. Chem.* **270,** 1107–1112
9. Saari, J. C. (1994) *Retinoids in Photosensitive Systems*, 2nd Ed., Raven Press, New York
10. Stecher, H., Gelb, M. H., Saari, J. C., and Palczewski, K. (1999) *J. Biol. Chem.* **274,** 8577–8585
11. Lyubarsky, A. L., Savchenko, A. B., Morocco, S. B., Daniele, L. L., Redmond, T. M., and Pugh, E. N., Jr. (2005) *Biochemistry* **44,** 9880–9888
12. Wenzel, A., Reme, C. E., Williams, T. P., Hafezi, F., and Grimm, C. (2001) *J. Neurosci.* **21,** 53–58
13. Chen, Y., Moiseyev, G., Takahashi, Y., and Ma, J. X. (2006) *FEBS Lett.* **580,** 4200–4204
14. Redmond, T. M., Poliakov, E., Yu, S., Tsai, J. Y., Lu, Z., and Gentleman, S. (2005) *Proc. Natl. Acad. Sci. U.S.A.* **102,** 13658–13663
15. Stecher, H., and Palczewski, K. (2000) in *Multienzyme Analysis of Visual Cycle* (Palczewski, K., ed), Academic Press, Pasadena, CA
16. Winston, A., and Rando, R. R. (1998) *Biochemistry* **37,** 2044–2050
17. Golczak, M., Kiser, P. D., Lodowski, D. T., Maeda, A., and Palczewski, K. (2010) *J. Biol. Chem.* **285,** 9667–9682
18. Chen, P., Hao, W., Rife, L., Wang, X. P., Shen, D., Chen, J., Ogden, T., Van Boemel, G. B., Wu, L., Yang, M., and Fong, H. K. (2001) *Nat. Genet.* **28,** 256–260
19. Wenzel, A., Oberhauser, V., Pugh, E. N., Jr., Lamb, T. D., Grimm, C., Samardzija, M., Fahl, E., Seeliger, M. W., Remé, C. E., and von Lintig, J. (2005) *J. Biol. Chem.* **280,** 29874–29884
20. Radu, R. A., Hu, J., Peng, J., Bok, D., Mata, N. L., and Travis, G. H. (2008) *J. Biol. Chem.* **283,** 19730–19738
21. Bok, D., Ruiz, A., Yaron, O., Jahng, W. J., Ray, A., Xue, L., and Rando, R. R. (2003) *Biochemistry* **42,** 6090–6098
22. Kamei, S., Chen-Kuo-Chang, M., Cazevieille, C., Lenaers, G., Olichon, A., Belenguer, P., Roussignol, G., Renard, N., Eybalin, M., Michelin, A., Delettre, C., Brabet, P., and Hamel, C. P. (2005) *Invest. Ophthalmol. Vis. Sci.* **46,** 4288–4294
23. Jin, M., Li, S., Moghrabi, W. N., Sun, H., and Travis, G. H. (2005) *Cell* **122,** 449–459
24. Lewis, S. E., Listenberger, L. L., Ory, D. S., and Schaffer, J. E. (2001) *J. Biol. Chem.* **276,** 37042–37050
25. Gu, S. M., Thompson, D. A., Srikumari, C. R., Lorenz, B., Finckh, U., Nicoletti, A., Murthy, K. R., Rathmann, M., Kumaramanickavel, G., Denton, M. J., and Gal, A. (1997) *Nat. Genet.* **17,** 194–197
26. Marlhens, F., Bareil, C., Griffoin, J. M., Zrenner, E., Amalric, P., Eliaou, C., Liu, S. Y., Harris, E., Redmond, T. M., Arnaud, B., Claustres, M., and Hamel, C. P. (1997) *Nat. Genet.* **17,** 139–141
27. Silva, E., Dharmaraj, S., Li, Y. Y., Pina, A. L., Carter, R. C., Loyer, M., Traboulsi, E., Theodossiadis, G., Koenekoop, R., Sundin, O., and Maumenee, I. (2004) *Ophthalmic Genet.* **25,** 205–217
28. Kiser, P. D., Golczak, M., Lodowski, D. T., Chance, M. R., and Palczewski, K. (2009) *Proc. Natl. Acad. Sci. U.S.A.* **106,** 17325–17330
29. Schaffer, J. E., and Lodish, H. F. (1994) *Cell* **79,** 427–436
30. Coe, N. R., Smith, A. J., Frohnert, B. I., Watkins, P. A., and Bernlohr, D. A. (1999) *J. Biol. Chem.* **274,** 36300–36304
31. Hall, A. M., Smith, A. J., and Bernlohr, D. A. (2003) *J. Biol. Chem.* **278,** 43008–43013
32. Hirsch, D., Stahl, A., and Lodish, H. F. (1998) *Proc. Natl. Acad. Sci. U.S.A.* **95,** 8625–8629
33. Martin, G., Nemoto, M., Gelman, L., Geffroy, S., Najib, J., Fruchart, J. C., Roevens, P., de Martinville, B., Deeb, S., and Auwerx, J. (2000) *Genomics* **66,** 296–304
34. Schmuth, M., Ortegon, A. M., Mao-Qiang, M., Elias, P. M., Feingold, K. R., and Stahl, A. (2005) *J. Invest. Dermatol.* **125,** 1174–1181
35. Fisher, S., Doherty, F., and Rowe, C. E. (1982) *Deacylation and Acylation of Phospholipids in Nervous Tissue*, Raven Press, New York
36. García-Martínez, C., Marotta, M., Moore-Carrasco, R., Guitart, M., Camps, M., Busquets, S., Montell, E., and Gómez-Foix, A. M. (2005) *Am. J. Physiol. Cell Physiol.* **288,** C1264–C1272
37. Milger, K., Herrmann, T., Becker, C., Gotthardt, D., Zickwolf, J., Ehehalt, R., Watkins, P. A., Stremmel, W., and Füllekrug, J. (2006) *J. Cell Sci.* **119,** 4678–4688
38. Saari, J. C., and Bredberg, D. L. (1989) *J. Biol. Chem.* **264,** 8636–8640
39. Saari, J. C., Bredberg, D. L., and Farrell, D. F. (1993) *Biochem. J.* **291,** 697–700
40. Kim, J. W., and Dang, C. V. (2005) *Trends Biochem. Sci.* **30,** 142–150